

A Novel Augmented Railgun Using Permanent Magnets

**Masoud Asgari¹, Mohammad Bagher Heydari^{2,*}, Leila Gharib¹, Asghar Keshtkar¹,
Nilofar Jafari³, Mohsen Zolfaghari⁴**

¹ Electrical Engineering Group, Imam Khomeini International University (IKIU), Qazvin, Iran

^{2,*} Electrical Engineering Department, Iran University of Science and Technology (IUST), Tehran, Iran

³ School of advanced medical sciences, Tabriz University of Medical Sciences, Tabriz, Iran

⁴ Electrical Engineering Department, Tarbiat Modares University (TMU), Tehran, Iran

*corresponding author, E-mail: mo_heydari@elec.iust.ac.ir

Abstract

A novel augmented railgun using a permanent magnet is proposed in this paper. The effects of the permanent magnet on the magnetic field and distribution of current density have been investigated. High current densities in the railguns can lead to high local temperature and erosion of the rails. Therefore, the current densities in the rails and armature should be decreased without the reduction of the Lorentz force which is required for acceleration. For this purpose, augmentation of the magnetic field can be used as an effective method. The Finite Element Method (FEM) simulations have been applied in this article to analyze the performance of the railgun in the presence of the magnets. Two augmented railgun structures have been introduced to produce a constant external magnetic field. For both structures, augmented railgun characteristics are studied in comparison to the railgun without the augmentation. The results show that augmentation with permanent magnet increases railgun efficiency, especially in low current railguns. For pulse current source $I=30\text{kA}$, Lorentz force of the augmented railgun with four magnets is 2.02 times greater than the conventional railgun.

1. Introduction

The railgun is one of the main electromagnetic launchers that can accelerate a projectile to high velocity. In the railgun structure, a large amount of heat is produced by high current at the contact between the rails and the missile. The generated heat corrodes the contact surface of the projectile and increases friction by roughing the surface. Therefore, the efficiency of the railgun reduces strongly. It should be noted that efficiency of the railgun is defined as the ratio of the missile energy to input electrical energy. The most popular way to improve efficiency is increasing inductance gradient, which is determined by the geometry of railgun bore [1-3], rails materials [4] and dimensions [5, 6]. This factor is typically in the range of 0.4 to 0.7 $\mu\text{H/m}$, depending on the rail geometry.

For the past several years, many researchers have worked on

optimizing of the inductance gradient [6-8]. Using parallel augmented railgun is the famous method for lowering the current, without decreasing the force on the projectile [9-13]. In this technique, a circuit with its energy supply is added to the conventional (non-augmented) railgun to establish an additional magnetic field [9]. Hence, it increases the electromagnetic force on the projectile, without increasing the current in the armature [11-13]. A multi-turn railgun is another method to achieve a high L' in comparison to the simple railgun. To achieve this, an additional power system is required for parallel rails which increases the applied mechanical force to rails [9].

The applied Lorentz force on the armature, which arises from the interaction of the armature's passing current with the existing magnetic field, is proportional to the power of two input currents and the gradient inductance. By decreasing the current in the rails, this force reduces significantly. Therefore, railgun could not be used with low current and small dimensions. A permanent magnet can be applied as the augmentation system for the railgun with a relatively low current in the range of 10 kA. Since the magnetic field is constant, a great Lorentz force during the ascending or decaying phase of current can be generated [14]. In [14], the magnetic field of 0.5T has been utilized in a space between the rails, which is produced by the permanent magnet (Nd-Fe-40).

In this paper, a novel augmented railgun using permanent magnets is proposed to increase the magnetic field in a space between the rails, which enhances inductance gradient. This article is organized as follows. In section 2, the open magnetic circuit augmented railguns are introduced in detail. In these structures, permanent magnets are located in place with a non-magnetic frame. Also, a parametric study has been done in this section to determine the key parameters in designing the structures. Then, closed magnetic circuit structures for augmented railgun are designed in section 3. In this section, permanent magnet pole pieces mounted on the magnetic steel has been applied to close the magnetic circuit. Next, the new augmented structures designed in this article have been compared with conventional railguns in section 4. The results show that augmentation with a permanent magnet is an

effective method for increasing railgun efficiency, especially in low current railguns. Therefore, it is possible to have a small electromagnetic launcher with acceptable velocity. Finally, section 5 concludes the paper.

2. Open Magnetic Circuit of Augmented Railguns

In Figure 1, two proposed geometries of augmented railguns are illustrated. Rails are assumed to be copper with a conductivity of 5.8×10^7 S/m, height (H) of 2cm, width (W) of 0.5cm and the separation (S) of 1.5cm. Each magnet has a height (B) of 1cm and a width (A) of 2cm. Other parameters of proposed structures are $S' = 1\text{cm}$, $\theta = 30^\circ$ and the magnets are supposed to be neodymium-iron-boron (NdFe-35). It should be noted that these parameters are considered as default parameters throughout this paper.

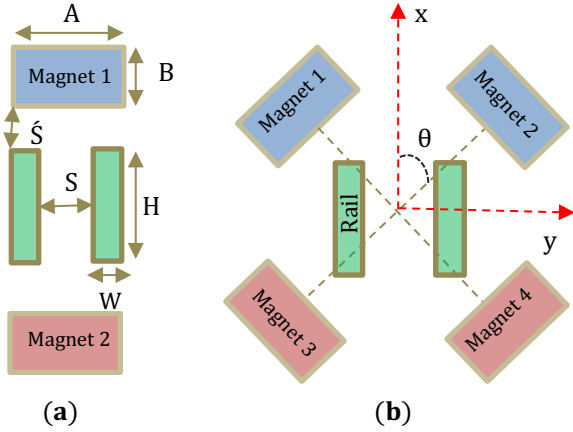


Figure 1: Two novel augmented railguns: (a) augmented railgun with 2 magnets (b) augmented railgun with 4 magnets.

2.1. Theory

Figure 2 illustrates the 3D schematic of augmented railgun with two magnets. In this figure, the external magnetic field (B_{ext}) is generated by two permanent magnets. By passing the current through the rails and closing the current-path by the armature, the total magnetic force (F_T) is applied on the armature, which can be expressed as:

$$\mathbf{F}_T = \mathbf{F}_{ext} + \mathbf{F}_R \quad (1)$$

Where F_{ext} , F_R are magnetic force applied on projectile arising from magnets and rail currents, respectively. The fundamental principle of the railgun is based on the Lorentz force for the current passing through the rails [15]:

$$\mathbf{F}_T = \iiint_V \mathbf{J} \times (\mathbf{B}_R + \mathbf{B}_{ext}) dV \quad (2)$$

Where \mathbf{J} represents the current distribution in the projectile and \mathbf{B}_R , \mathbf{B}_{ext} are the magnetic field of rails and external magnetic field, respectively.

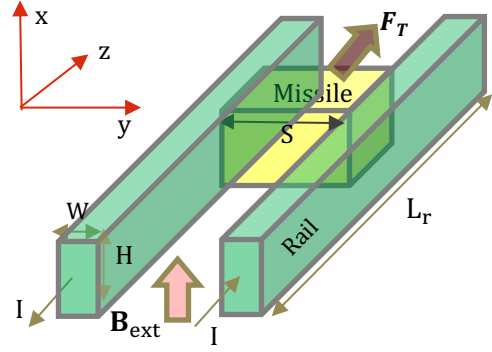


Figure 2: The 3D schematic of augmented railgun with two magnets

Let us calculate the amplitude of magnetic force produced by the magnets (F_{ext}) and the currents (F_R) separately. The magnetic force applied on the projectile by the rails can be written as [15]:

$$F_R = \frac{1}{2} \frac{\partial L}{\partial z} I^2 = \frac{1}{2} L' I^2 \quad (3)$$

Where L' is the inductance gradient and has been derived for the rectangular shape of the rails by J.F.Kerrisk in [16]:

$$L' = \mu_0 \left[\text{Ln} \left(1.007 + 2.74 \frac{S}{H} + 0.02 \frac{W}{H} + 0.26 \frac{W}{H} \frac{S}{H} \right) \right] \times \left[0.44 - 0.07 \times \text{Ln} \left(1 + 3.39 \frac{W}{H} - 0.06 \frac{W}{H} \frac{S}{H} \right) \right] \quad (4)$$

In above relation, S and I are the length of the armature and the rail currents, respectively. Also, the rail length is presumed to be long enough ($L_r \gg 1$) in J.F.Kerrisk calculations [16]. Now, for the magnetic force applied on the missile by the magnets, one can write:

$$F_{ext} = B_0 I S \quad (5)$$

Hence, the total Lorentz force for the augmented railgun with two permanent magnets can be expressed as:

$$F_T = \frac{1}{2} L' I^2 + B_0 I S \quad (6)$$

Where L' has been given in relation (4). To increase the Lorentz force in the conventional railgun (non-augmented with permanent magnets), high currents for the rails are utilized, which cause the thermal problems and erosion of rails. However, the relation (6) indicates that the Lorentz force is enhanced in the augmented railgun. For low currents, we deem that:

$$F_{ext} \gg F_R \Rightarrow B_0 \gg \frac{L' I}{2S} \quad (7)$$

This condition guarantees that the magnetic force applied on the projectile by the permanent magnets is dominant. Let us suppose that the friction is zero in the structure. Therefore, the projectile has a constant acceleration, which the acceleration

is derived by using Newton's first law:

$$a = \frac{F_T}{m} \approx \frac{F_{ext}}{m} = \frac{I S B_0}{m} \quad (8)$$

In above relation, m is the mass of the projectile. To enhance the magnetic field concentration in the armature region, we propose the augmented railgun with 4 magnets, which is similar to quadrupole magnets (Q-magnets) used in industry [17]. In this structure, the same poles have been located in the top or in the bottom of the railgun to focus and increase the field intensity in the armature region (for instance, two N-poles has been placed at the top of the structure), unlike the Q-magnets structure. Figure 3 shows the magnetic field distribution for the structure of Figure 1 (b). It is obvious that the magnetic field has been concentrated in the armature region and is uniform over there. The electromagnetic field relations for this structure (Figure 1(b)) is too complicate (like the relations for Q-magnets) and is outside the scope of this paper. Therefore, we only study the simulation results in this article and will show that the augmented railgun with four magnets has better performance than the augmented railgun with two magnets.

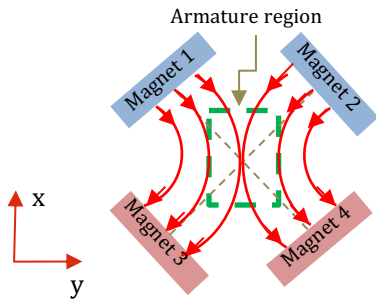


Figure 3: Side view of magnetic field distributions for structure of Figure 1(b)

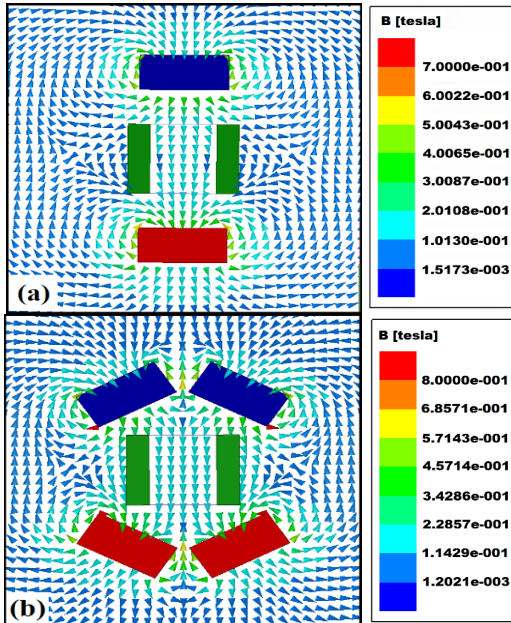


Figure 4: Magnetic flux lines for: (a) augmented railgun with 2 magnets. (b) Augmented railgun with 4 magnets.

The magnetic flux densities of magnets for both structures have been demonstrated in Figure 4. By using four magnets with an angle of 30° instead of two magnets for augmentation, the magnitude of the magnetic field in the armature region increases about % 65. In fact, the magnetic field in the armature region is enhanced without the rails current increment. This technique does not need to an additional power source for increasing total magnetic field and railgun efficiency, which it is the main advantage of this method.

2.2. Parametric Study

It is interesting to study the variations of the magnetic field intensity by the several factors. In both structures in Figure 1, the height (B) and width (A) of the magnets significantly influence the produced magnetic field in the armature region. Both structures are simulated for various quantities of the magnet height (B), whereas the other parameters are maintained fixed and equal to the default ones. The magnetic fields in the center of the coordinate system for both structures are calculated and plotted in Figure 5. One can see from this figure that the magnetic field increases as the magnets height (B) enhances.

The width of the permanent magnets also has a considerable effect on the magnitude of the magnetic fields. The magnetic field intensity versus the width (A) of permanent magnets has been plotted in Figure 6 for both structures. By altering the width of the magnets, produced magnetic field varies in a wide range. To concentrate the magnetic fields in the armature region, the width of permanent magnets must be increased, but the produced magnetic field tends to be constant for greater widths, due to the constant magnetic field strength of the permanent magnets. Furthermore, it should be noted that the maximum width of the magnets is 4cm because the magnets will be intersected with each other as the width increases in the structure of Figure 1(b). For simplicity, it is assumed that $\theta = 45^\circ$ in Figure 6.

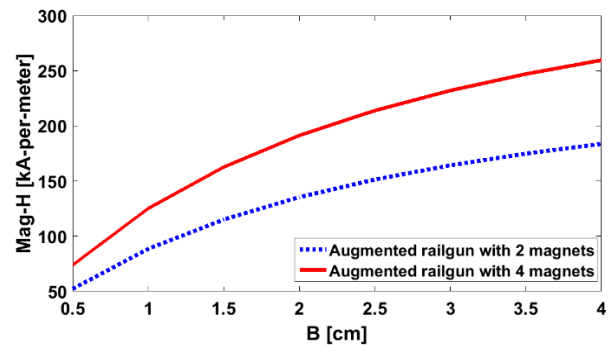


Figure 5: Magnetic field intensity versus the height (B) of permanent magnets: blue dashed line and red solid line are for the railgun structures of Figure 1 (a), (b), respectively.

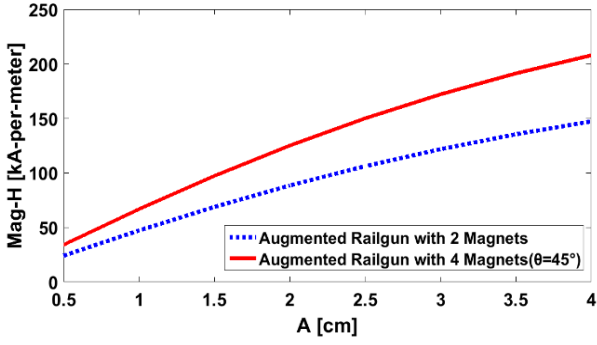


Figure 6: Magnetic field intensity versus the width (A) of permanent magnets: blue dashed line and red solid line are for the railgun structures of Figure 1 (a), (b), respectively.

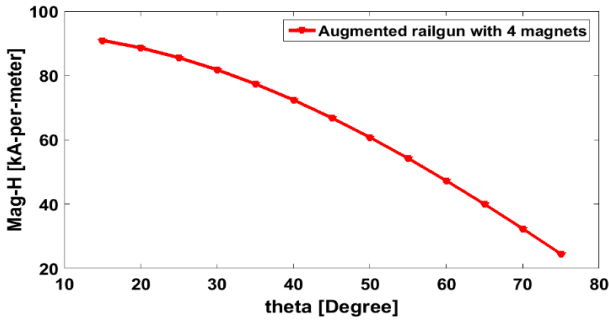


Figure 7: Magnetic field intensity of permanent magnet structure with four magnets versus oblique angles.

It is important to emphasize that the oblique angle (θ) in the augmented railgun with four magnets, affects on the magnetic field of the magnets. In this case, the permanent magnet width (A), is taken equal to 1 cm for the convenience of simulations. Variations of produced magnetic field versus the oblique angle in the origin of the coordinate system for the augmented railgun with four magnets are displayed in Figure 7. It can be seen that by increasing the oblique angle (θ) from 15° to 75° , the magnetic field is reduced about 3.7 times. The maximum value of $90.71 \text{ A}\cdot\text{m}^{-1}$ is obtained for at the angle of 15 degree which is 1.91 times greater than the produced magnetic field in the augmented railgun with two magnets. Therefore, by utilizing the augmented railgun with four magnets, the produced magnetic field increases remarkably.

3. Closed Magnetic Circuit of Augmented Railguns

In the previous section, we designed the augmented railguns with permanent magnets. The fields produced by these magnets are concentrated on the edge sides. This matter happens because there is a high reluctance in the middle of the magnets and thus the magnetic flux tends to close its path in shorter way. To overcome this problem, the steel has been used on the top and bottom of our proposed railguns to produce homogenous magnetic field.

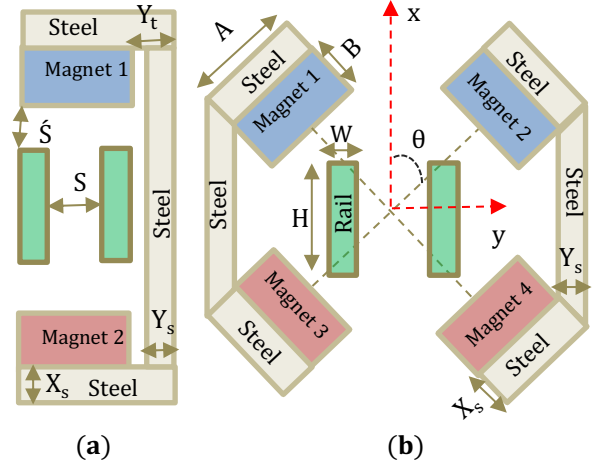


Figure 8: Structures of closed magnetic circuits: (a) augmented railgun with 2 magnets. (b) Augmented railgun with 4 magnets.

The magnetic circuit consists of a high permeability steel (1010), neodymium permanent magnets (NdFe-35) and the railgun barrel air gap (where the armature moves inside it). The design configurations of the closed magnetic circuit for both augmented railgun structures are shown in Figure 8.

The parameters of the proposed configurations are $Y_s = 0.55 \text{ cm}$, $X_s = Y_t = 1 \text{ cm}$ and other parameters are maintained constant. Like the Open magnetic circuit of augmented railguns, the 2-D planar model has been used instead of the 3-D circuit to simplify and reduces the huge numbers of meshes required for the Maxwell ANSYS program.

Let us assume that the permanent magnet operates in the state represented by the maximum value of BH_{max} . Therefore, the minimum permanent magnet volume (V_{PM}) for generating a flux density (B_{gap}) in the volume of the barrel air gap (V_{gap}), is obtained by [18]:

$$V_{PM} = \frac{B_{gap} V_{gap}}{\mu_0 (BH_{max})} \quad (9)$$

Where B_{gap} and BH_{max} are the magnetic flux density of the air gap and the maximum amount of the permanent magnet, respectively. Equation (9) indicates that large flux density in the air-gap can be obtained by reducing the air-gap volume. However, this cannot be obtained in practical applications because the magnetic core saturates as the flux density increases beyond a given point.

The magnetic field distributions for both closed magnetic circuit of augmented railguns are displayed in Figure 9. This figure shows that the magnetic field increases considerably in the armature region by using the closed circuit configurations. Therefore, in comparison with open circuit structures, magnetic field intensity enhances about 30% in the closed-circuit structures. In Figure 9(b), it is obvious that the magnetic flux density in the armature region of $1.5 \text{ cm} \times 2 \text{ cm}$ is about 0.4T. In [14], the magnetic flux density of 0.53T in the armature region of about $5 \text{ mm} \times 5 \text{ mm}$ is reported. To

compare this result with [14], we achieved approximately the same magnetic flux density in 12 times bigger armature area. Therefore, this railgun can be applied for large missiles.

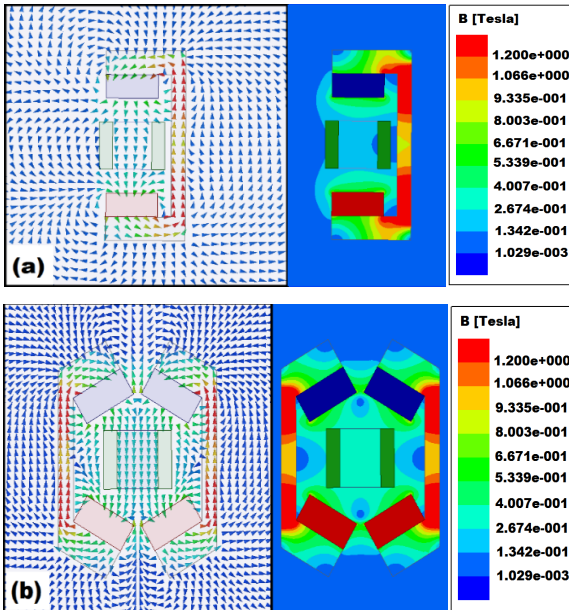


Figure 9: Magnetic flux density for: (a) augmented railgun with 2 magnets. (b) Augmented railgun with 4 magnets.

4. Comparison between Permanent Magnet Augmented Railgun and Conventional Railgun

In this section, a comparison between the permanent magnet augmented railguns with conventional railguns will be done. It is assumed that the primary current through the rails is 10 kA. The direction of current in the rails is determined according to the direction of the external magnetic field in the armature region. It is desirable that the magnetic fields of the permanent magnets and magnetic fields of the rails have the same direction (along the X-axis) in the armature region.

In Figure 10, the magnetic flux density for the conventional and permanent magnet augmented railguns are shown in the armature region. It can be observed from this figure that magnetic field increases in the armature region. According to the symmetry in the structures and applied boundary condition of the electric wall to the X-Z plane, the current density distributions are shown only in the first quadrant.

Figure 11 illustrates the current density on the cross section of rail in all cases. It is obvious that conventional and augmented permanent magnet railguns approximately have the same current distributions. Therefore, the magnets do not have a significant effect on current distribution of the rails.

To calculate the accurate value of Lorentz force exerted on the armature, three-dimensional simulations can be performed for the structures which are shown in Figure 10. In both structures in Figure 12, the simulated rails and armature are copper bars with 5mm thickness and 2cm width. The rails length is 50cm, the armature height is 2cm, and the distance between the armature and the launcher rear end is 25cm. The

Lorentz force of the armature for different amounts of the pulse current sources have been simulated in three dimensions and results are given in Table 1. This table demonstrates that the Lorentz force in the direction of the armature motion is increased in all cases due to the external magnetic field.

Table 1 expresses that the armature Lorentz force decreases significantly by reducing the rails current, as expected in equation (6). Minimum percent of increment in the armature Lorentz force is obtained in $I=100\text{kA}$ for the permanent magnet augmentation in comparison with the conventional railgun. In $I=30\text{kA}$, Lorentz force of the augmented railgun with four magnets is 2.02 times greater than the conventional railgun. As a result, augmentation with the permanent magnet is an effective method for increasing railgun efficiency, especially in low current railguns. Therefore, it is possible to have a smaller caliber electromagnetic launcher with acceptable velocity by using the permanent magnet for the augmented railgun.

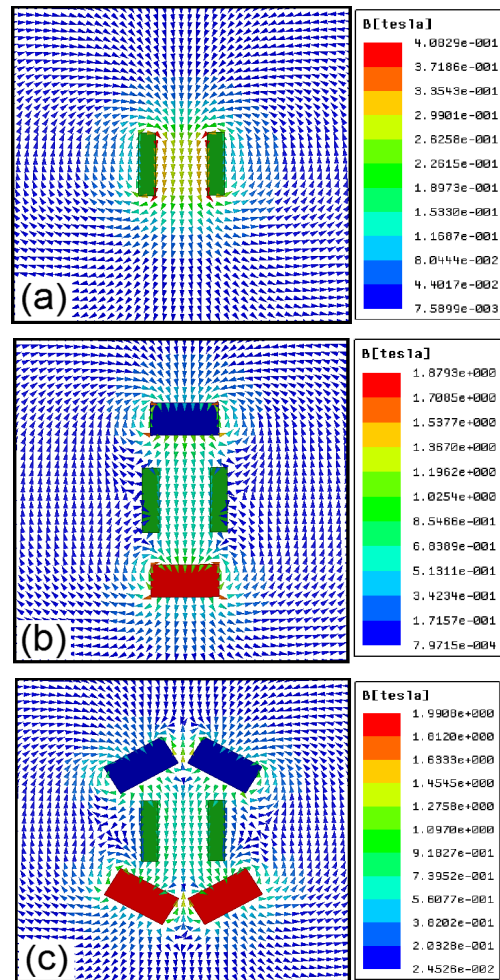


Figure 10: Magnetic flux density for: (a) Conventional railgun. (b) Augmented railgun with 2 magnets. (c) Augmented railgun with 4 magnets.

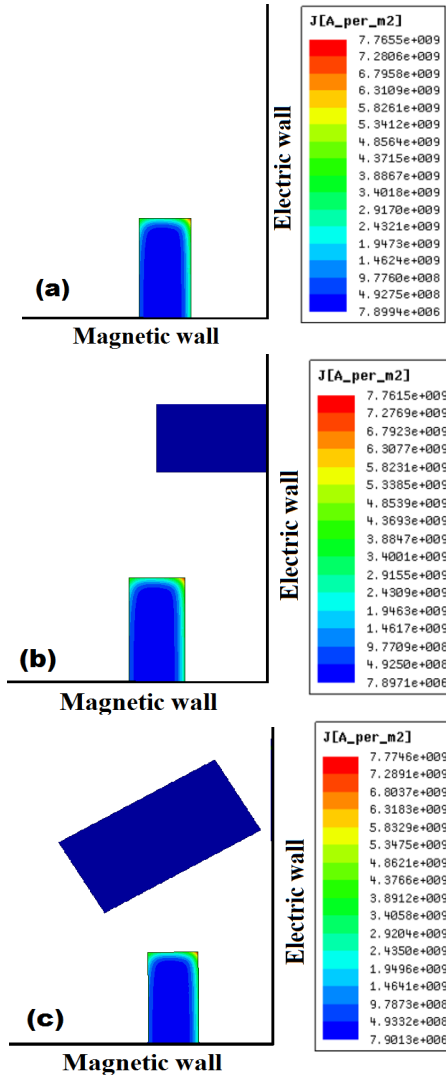


Figure 11: Current distributions on rail for: (a) conventional railgun (b) Augmented railgun with 2 magnets. (c) Augmented railgun with 4 magnets.

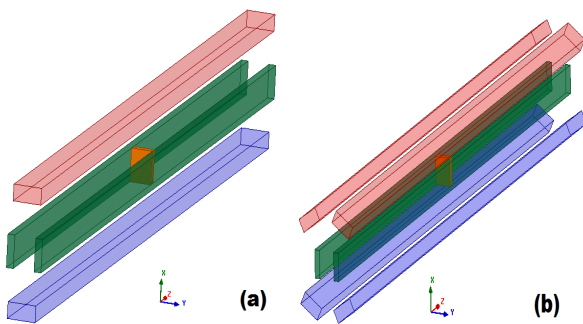


Figure 12: Three-dimensional structures of the permanent magnet augmented railgun: (a) augmented railgun with 2 magnets. (b) Augmented railgun with 4 magnets.

Table 1: Armature Lorentz force (kN) versus the pulse current sources.

pulse current sources (kA)	Conventional railgun	Augmented railgun with 2 magnets	Augmented railgun with 4 magnets ($\theta=30^\circ$)
30	0.185	0.267	0.373
100	2.05	2.36	2.81
200	8.23	8.91	10.03
300	18.52	19.34	21.75
400	32.93	34.23	37.87

5. Conclusions

In this paper, novel augmented railgun using permanent magnets was designed to increase the magnetic field in a space between the rails. First, the open magnetic circuit augmented railgun structures are introduced. In these structures, permanent magnets have been located in place with a non-magnetic frame. Next, a parametric study was done, and the key parameters of the designed structures for the magnets was studied in detail. Then, closed magnetic circuit structures for augmented railgun were offered. A comparison between the conventional railgun and new augmented railgun structures showed that augmentation with the permanent magnet is an effective method for increasing railgun efficiency, especially in low current railguns. For pulse current source $I=30\text{kA}$, Lorentz force of the augmented railgun with four magnets is 2.02 times greater than the conventional railgun. Furthermore, we showed that the magnetic flux density in the armature region of $1.5\text{cm} \times 2\text{cm}$ is about 0.4T in our novel railguns. In [14], the magnetic flux density of 0.53T is reported in the armature region of $5\text{mm} \times 5\text{mm}$. Therefore, we achieved approximately the same magnetic flux density in 12 times bigger armature area.

References

- [1] N. Sengil, "Implementation of Monte Carlo method on electromagnetic launcher simulator," *IEEE Transactions on Plasma Science*, vol. 41, pp. 1156-1160, 2013.
- [2] R. A. Marshall, "Railgun bore geometry, round or square?," *IEEE transactions on magnetics*, vol. 35, pp. 427-431, 1999.
- [3] M. S. Bayati and A. Keshtkar, "Study of the current distribution, magnetic field, and inductance gradient of rectangular and circular railguns," *IEEE Transactions on Plasma Science*, vol. 41, pp. 1376-1381, 2013.
- [4] A. Keshtkar, S. Bayati, and A. Keshtkar, "Effect of rail's material on railgun inductance gradient and losses," in *Electromagnetic Launch Technology, 2008 14th Symposium on*, 2008, pp. 1-4.
- [5] A. Keshtkar, S. Bayati, and A. Keshtkar, "Derivation of a formula for inductance gradient using intelligent estimation method," *IEEE Transactions on Magnetics*, vol. 45, pp. 305-308, 2009.
- [6] A. Keshtkar, "Effect of rail dimension on current distribution and inductance gradient," *IEEE Transactions on Magnetics*, vol. 41, pp. 383-386, 2005.

- [7] B.-K. Kim and K.-T. Hsieh, "Effect of rail/armature geometry on current density distribution and inductance gradient," *IEEE transactions on Magnetics*, vol. 35, pp. 413-416, 1999.
- [8] T. Watt and F. Stefani, "Experimental and computational investigation of root-radius melting in C-shaped solid armatures," *IEEE transactions on magnetics*, vol. 41, pp. 442-447, 2005.
- [9] J. Gallant, "Parametric study of an augmented railgun," *IEEE Transactions on Magnetics*, vol. 39, pp. 451-455, 2003.
- [10] D. Fikse, J. Ciesar, H. Wehrli, H. Riemersma, E. Docherty, and C. Pipich, "The HART I augmented electric gun facility," *IEEE transactions on magnetics*, vol. 27, pp. 176-180, 1991.
- [11] J. Gallant and P. Lehmann, "Experiments with brush projectiles in a parallel augmented railgun," in *Electromagnetic Launch Technology, 2004. 2004 12th Symposium on*, 2005, pp. 53-58.
- [12] T. G. Engel, M. J. Veracka, J. M. Neri, and C. N. Boyer, "Design of low-current high-efficiency augmented railguns," *IEEE Transactions on Plasma Science*, vol. 37, pp. 2385-2389, 2009.
- [13] A. Keshtkar, L. Gharib, M. S. Bayati, and M. Abbasi, "Simulation of a two-turn railgun and comparison between a conventional railgun and a two-turn railgun by 3-D FEM," *IEEE Trans. Plasma Sci.*, vol. 41, pp. 1392-1397, 2013.
- [14] S. Katsuki, H. Akiyama, N. Eguchi, M. Sued, M. Soejima, T. Maeda, *et al.*, "Behaviors of plasma armature in the augmented railgun using a permanent magnet," *IEEE transactions on magnetics*, vol. 31, pp. 183-188, 1995.
- [15] R. A. Marshall and W. Ying, *Railguns: their science and technology*: China Machine Press, 2004.
- [16] J. Kerrisk, "Current distribution and inductance calculations for rail-gun conductors," 1981.
- [17] J. Coey, "Permanent magnet applications," *Journal of Magnetism and Magnetic Materials*, vol. 248, pp. 441-456, 2002.
- [18] A. Sitzia, "Book Review: Permanent Magnets in Theory and Practice," ed: SAGE Publications Sage UK: London, England, 1989.